

A diffuse bubble-like radio-halo source MRC 0116+111: imprint of AGN feedback in a low-mass cluster of galaxies

Joydeep Bagchi,¹★ Joe Jacob,² Gopal-Krishna,³ Norbert Werner,⁴ Nitin Wadnerkar,⁵ Jaydeep Belapure⁶ and A. C. Kumbharkhane⁵

¹Inter University Center for Astronomy and Astrophysics (IUCAA), Post Bag 4, Ganeshkhind, Pune 411 007, India

²Department of Physics, Newman College, Thodupuzha 685 585, India

³National Center for Radio Astrophysics (NCRA-TIFR), Post Bag 3, Ganeshkhind, Pune 411 007, India

⁴Kavli Institute for Particle Astrophysics and Cosmology, Stanford University, 452 Lomita Mall, Stanford, CA 94305, USA

⁵School of Physical Sciences, Swami Ramanand Teerth Marathwada University, Nanded 431 606, India

⁶Department of Physics, Pune University, Pune 411 007, India

Accepted 2009 June 24. Received 2009 June 22; in original form 2009 May 7

ABSTRACT

We present detailed observations of MRC 0116+111, revealing a luminous, miniradio halo of ~ 240 -kpc diameter located at the centre of a cluster of galaxies at redshift $z = 0.131$. Our optical and multiwavelength Giant Metrewave Radio Telescope and Very Large Array radio observations reveal a highly unusual radio source: showing a pair of giant (~ 100 -kpc diameter) bubble-like diffuse structures, that are about three times larger than the analogous extended radio emission observed in M87 – the dominant central radio galaxy in the Virgo cluster. However, in MRC 0116+111 we do not detect any ongoing active galactic nucleus (AGN) activity, such as a compact core or active radio jets feeding the plasma bubbles. The radio emitting relativistic particles and magnetic fields were probably seeded in the past by a pair of radio jets originating in the AGN of the central cD galaxy. The extremely steep high-frequency radio spectrum of the north-western bubble, located ~ 100 kpc from cluster centre, indicates radiation losses, possibly because having detached, it is rising buoyantly and moving away into the putative hot intracluster medium. The other bubble, closer to the cluster centre, shows signs of ongoing particle re-acceleration. We estimate that the radio jets which inflated these two bubbles might have also fed enough energy into the intracluster medium to create an enormous system of cavities and shock fronts, and to drive a massive outflow from the AGN, which could counter-balance and even quench a cooling flow. Therefore, this source presents an excellent opportunity to understand the energetics and the dynamical evolution of radio jet inflated plasma bubbles in the hot cluster atmosphere.

Key words: acceleration of particles – magnetic fields – galaxies: active – galaxies: clusters: individual: MRC 0116+111 – radio continuum: general – X-rays: galaxies: clusters.

1 INTRODUCTION

Multiwavelength observations of galaxy clusters have provided substantial evidences for supermassive black holes (SMBHs) residing in the nuclei of giant elliptical galaxies which are found near the cluster centres and dense galactic environments. The extremely large mass of these black holes ($M_{\text{bh}} \sim 10^6$ – $10^9 M_{\odot}$) raises several questions: what processes regulate the growth of these SMBH? why and how only some of them turn-on their radio jets? What is the source of fuel for the central engine? and what environmental

impact could a massive black hole and its energetic outflows may have on the host galaxy and the surrounding gaseous intracluster medium (ICM)? Some important clues to these questions are provided by radio and X-ray observations of galaxy clusters which show that majority (as many as ~ 70 – 100 per cent) of these central giant elliptical galaxies (cD galaxies) may become radio loud – ejecting plasma and magnetic fields in the form of powerful radio jets – when they are located at the focus of a ‘cooling flow’ (Burns 1990; Bagchi & Kapahi 1994; Mittal et al. 2009). The probability of finding a central radio source increases in direct proportion to decrease in cooling time of the inner ICM (Bagchi & Kapahi 1994; Mittal et al. 2009). A cooling flow is established when the central radiative cooling time (t_{cool}) of the ICM of a galaxy cluster is quite

*E-mail: joydeep@iucaa.ernet.in

short ($t_{\text{cool}} \lesssim 1$ Gyr $\ll H_0^{-1}$, the Hubble time). In the absence of a central heating mechanism, the pressure balance is disturbed and to restore the hydrostatic equilibrium, a steady convergent flow of cooling gas towards the cluster centre is setup, in which the gas cools below the X-ray temperature and accretes on to the central elliptical galaxy (Fabian 1994; Peterson & Fabian 2006).

Strongest spectral signatures of this cooling gas are low-energy X-ray lines below 1 keV from various ionization states of iron (mainly Fe L complex). Early *Einstein* observations of nearby radio-loud cD galaxies in cooling-flow clusters such as M87 (Virgo A) and NGC 1275 (3C 84, Perseus A) did find the expected Fe L lines, thus supporting the cooling model (Canizares et al. 1982). Evidence for cooling gas was also seen in other wavelengths, although at rates lower than expected; H α emitting filaments of ionized, warm gas (Heckman 1981), star formation activity (McNamara & O'Connell 1989) and radio observations of CO molecular lines (Edge 2001; Salome et al. 2008).

In recent years more detailed X-ray observations with *Chandra* and *XMM-Newton* telescopes have revealed a surprising and somewhat puzzling aspect of cooling flows; they showed far less cooling below X-ray emitting temperatures than expected, altering the previously accepted picture of cooling flows (cf. review by Peterson & Fabian 2006). Unless gas is thermally supported, radiative cooling leads to a ‘cooling catastrophe’, i.e. an inexorable inflow of cold gas on to the central galaxy. To prevent this, some heating mechanism was required to raise gas temperature above ~ 2 keV, suppressing the cooling flow. Although several such mechanisms were discussed, the most promising heating process turned out to be the energy injected into the ICM by powerful radio jets emanating from active galactic nuclei (AGN) in central galaxies of clusters and groups (e.g. Binney & Tabor 1995; Churazov et al. 2001, 2002; Bruggen & Kaiser 2002, and see McNamara & Nulsen 2007 for a review). This AGN-heating mechanism is also found to be particularly effective in suppressing the star formation activity, that one expects to be prolific around the brightest cluster galaxies (BCGs) due to their preferential location in clusters. These BCGs should be accompanied by intense star formation activity and have blue colours, neither of which is observed and energy input from AGN outbursts in clusters may be especially needed to explain the observations.

One of the canonical models of AGN posits accretion of gaseous medium as fuel for the nuclear black hole, such that AGN outflows are powered by gravitational binding energy released by the infalling matter (Begelman, Blandford & Rees 1984). The observed strong association of an AGN in the central galaxy and the surrounding cooling core lends good support to this model, which suggests that the black hole ‘central engine’ is possibly fuelled by accretion of cooling gas (Bagchi & Kapahi 1994; Allen et al. 2006; Mittal et al. 2009), with the flow rate self-regulated by AGN heating (Churazov et al. 2001; Cattaneo & Teyssier 2007), indicating a complex feedback loop with tight coupling between a central black hole and the surrounding gas of cooling core. Although this model is plausible and widely used, many details of how this feedback process works remain far from clear.

When the radio jets emerging from the central black hole (AGN) interact with the dense thermal plasma of the ICM, two bubble-like lobes of non-thermal plasma are inflated, which are filled with relativistic particles and magnetic field and thus become visible in radio observations. Such bubbles were first proposed by Gull & Northover (1973) and later identified in several clusters using radio and X-ray observations (see McNamara & Nulsen 2007). The most clear example of this phenomenon is the non-thermal

bubbles in clusters MS 0735.6+7421, Hydra A, Abell 2052, Perseus and others, showing an unusually large and energetic pair of radio emitting, X-ray dark cavities (e.g. McNamara et al. 2000, 2005; Blanton et al. 2003; McNamara & Nulsen 2007; Wise et al. 2007). Episodic (on-off) activity of radio jets injects non-thermal radio bubbles which may heat the ICM via weak shocks, and additionally these plasma bubbles are responsible for the mechanical (PdV) work done on the ICM for heating it, which is one of the favoured mechanism of AGN–ICM feedback.

Several examples of these bubble and cavities, with diameter ranging from 1 to 100 kpc, have been found in the hot atmosphere surrounding galaxies in groups and clusters (e.g. Birzan et al. 2004; Dunn & Fabian 2004). In few sources the energy involved is $\sim 10^{60-62}$ erg, the most powerful radio outbursts known (e.g. McNamara et al. 2005; McNamara & Nulsen 2007). The energy involved is large enough to strongly affect or even quench any cooling flow, and to drive large-scale outflows that redistribute and heat the gas on cluster-wide scales. The radio lobe plasma fill the cavities, which shows that expanding jets have displaced the ICM thermal gas, excavating X-ray dark cavities and possibly shock heating the surrounding gaseous medium (e.g. McNamara et al. 2000, 2005; Fabian et al. 2003). This heat input into the ICM may be large enough to counter-balance the cooling loss, and may even stop the accretion flow of matter on to the SMBH, thus starving the central engine of its fuel. Therefore, bubble-like diffuse radio sources residing near cluster centres are extremely effective probes of the poorly understood physics of the radio-galaxy–ICM feedback process.

Also directly related to these issues is the detection of diffuse non-thermal synchrotron radio plasma and magnetic fields mixed with the ICM of clusters. Approximately 30 galaxy clusters show giant radio haloes – centrally located synchrotron radiation extended on mega-parsec scales with a regular morphology, similar to that observed in X-rays. A few galaxy clusters also show peripherally located radio relics which have elongated morphology and that may extend over 100 kpc–1 Mpc scales. The radio emission from giant radio haloes and radio relics is not directly connected to the galaxies in clusters and both are mainly observed in merging clusters, which indicates that radio emitting relativistic electrons may have been accelerated *in situ* in merger-induced shocks and/or turbulence (cf. review Ferrari et al. 2008 and references therein). In the case of relics, an alternative model has been proposed, which invokes adiabatic compression of relic radio lobes by cluster merger shocks (Ensslin & Gopal-Krishna 2001).

A third remarkable category of large-scale diffuse radio sources are the radio minihaloes. Unlike the mega-parsec scale giant radio haloes and relics (which are found to be associated with cluster merger phenomenon and hence rarely found in cooling core clusters), radio minihaloes are not only a few times smaller in size ($\sim 100-500$ kpc, comparable to size of the cooling core) but also they are seen to surround the central radio galaxies of some cooling core clusters (see reviews Feretti & Giovannini 2008; Ferrari et al. 2008). Radio minihaloes are rare objects, have low surface brightness and a steep spectral index ($\alpha \lesssim -1$).¹ The fact that minihaloes are mostly observed at the centres of cooling-core clusters indicates that their origin and evolution are connected to the energy feedback from the central AGN into the ICM via radio jets and cooling/heating processes. Thus, while minihaloes share with giant haloes and relics the properties of a steep radio spectrum and very

¹ We use definition: flux density (S_ν) \propto frequency (ν) $^\alpha$.

low surface brightness, their physical origins are probably different. This is corroborated by the finding that unlike the minihaloes, giant haloes have remarkably similar synchrotron emissivities, albeit the two are similar morphologically (Murgia et al. 2009). Radio minihaloes are still a very poorly understood phenomenon and in observational terms, they being roughly centred at the dominant cluster radio galaxy makes their detection particularly challenging. Three early examples of radio minihaloes are associated with the cooling flow clusters: Perseus A (Pedlar et al. 1990), A2142 (Giovannini & Feretti 2000) and RXJ1347.5–1145 (Gitti et al. 2007). Continued searches have so far revealed no more than 10 minihaloes (see Feretti & Giovannini 2008; Ferrari et al. 2008 and references therein). Because of their very steep spectrum, radio haloes in clusters are difficult to detect at higher frequencies, and therefore a low-frequency radio telescope such as the Giant Metrewave Radio Telescope (GMRT) is well suited for their study (e.g. Brunetti et al. 2008; Venturi et al. 2008).

The focus of present paper is on a diffuse halo-like radio source MRC 0116+111 and its radio and optical properties, as revealed in our detailed observations, their astrophysical implications and impact on the above topics. Earlier a brief report on this radio source matching the characteristics of a minihalo was presented by some of us, based on Very Large Array (VLA) and GMRT observations (Gopal-Krishna et al. 2002). These radio observations revealed an amorphous source of an ultrasteep radio spectrum ($\alpha \sim -1.3$) and size ~ 1.5 arcmin. This Molonglo Reference Catalogue source MRC 0116+111 had been resolved on arcmin scale in the Ooty Lunar Occultation Survey at 327 MHz (Joshi & Singal 1980). An R-band image taken with the European Southern Observatory (ESO) New Technology Telescope (NTT) showed that this amorphous radio source is centred at the dominant member of a galaxy group having at least three–four members for which NTT/EMMI (ESO Multi-Mode Instrument) spectroscopy yielded redshifts close to 0.131 (Gopal-Krishna et al. 2002). More recently, this system has been listed in a catalogue of distant clusters of galaxies (Lopes et al. 2004). In order to clarify the nature of this peculiar radio source and its relation to the brightest cluster galaxies, we have imaged it freshly with GMRT at 240, 621 MHz and 1.28 GHz with high sensitivity and resolution, and have also carried out an improved analysis of the existing VLA snapshot data at 1.4 and 4.8 GHz. Additionally, we have taken its deep *B*, *V*, *R*, *I* CCD images with the 2-m optical telescope located at the IUCAA Girawali Observatory (IGO), Pune, India.

In this work we have used a Hubble constant $H_0 = 70 \text{ km}(\text{s Mpc})^{-1}$, and Λ cold dark matter (Λ CDM) ‘concordance’ cosmology with $\Omega_M = 0.27$ and $\Omega_\Lambda = 0.73$, which results in a luminosity distance $D_L = 617.2 \text{ Mpc}$, and linear scale of $2.34 \text{ kpc arcsec}^{-1}$ for a redshift $z = 0.131$ of MRC 0116+111.

2 OBSERVATIONS AND DATA ANALYSIS

2.1 Radio observations

Multifrequency GMRT² observations were carried out on 2007 December 1 and 2 at 1.28 GHz ($\lambda = 23.4 \text{ cm}$), 621 MHz ($\lambda = 48.3 \text{ cm}$) and 240 MHz ($\lambda = 125 \text{ cm}$) using the 128 channel FX correlator. GMRT is an earth-rotation aperture-synthesis array of 30 telescopes operating in 150–1420 MHz range (Swarup et al. 1991).

² The GMRT is a national facility operated by the National Centre for Radio Astrophysics of the TIFR, India.

The data were recorded in the spectral-line mode with 128 channels per sideband, resulting in a spectral resolution of 125 kHz per channel. The 621- and 240-MHz observations were taken simultaneously with the co-axial dual-band feed system of GMRT. At 240 MHz we used a bandwidth of only 6 MHz out of total 16 MHz available in one sideband (USB), and at 621 MHz full bandwidth of 16 MHz in one sideband (USB) was used. At 621 MHz only the right-handed circular polarization (RR) and at 240 MHz only the left-handed circular polarization (LL) was recorded. Both right and left circular polarization (RR, LL) data were recorded at 1.28 GHz, and bandwidth of 16 MHz was used in one sideband (USB). During each observing run a sequence of ~ 20 - to 30-min scans of the source were taken, interspersed with the VLA phase calibrator 0204+152 (4C +15.05). The telescope gain, bandpass response and flux density scale were calibrated by observing the primary flux density calibrator 3C 48, and boot strapping the flux density scale to the standard ‘Baars-scale’ (Baars et al. 1977). After excising faulty data and radio-frequency interference (RFI), mainly affecting low-frequency observations, the calibrated data were transformed into the image plane using the standard routines in AIPS, including a few cycles of self-calibration. By applying suitable tapers to the visibilities, final maps with synthesized Gaussian beams of full width at half-maximum (FWHM) ranging 5 to 6 arcsec at 1280 and 621 MHz, and ~ 10 arcsec at 240 MHz were obtained (see Figs 1 and 7).

The first of VLA³ observations took place on 1992 June 22 in C band (DnC array configuration, 4.88 and 4.83 GHz centre frequencies, using two IFs of 50 MHz BW each). The total integration time on MRC 0116+111 was about 10 min and VLA calibrator B0235+164 was used for phase calibration. VLA calibrator 3C 48 was also observed for amplitude calibration. The second VLA observation was made on 1997 June 12 in L band (CnB configuration, 1.46 and 1.38 GHz centre frequencies, using two IFs of 50 MHz BW each). The total on-source integration time was about 38 min and VLA flux calibrator 3C 48 was used for both amplitude and phase calibrations. For data reduction we used standard routines available in AIPS software. Further editing, and imaging with a few cycles of self-calibration resulted in good quality radio maps. After deconvolution, the final maps were restored with synthesized Gaussian beams of FWHM 12 arcsec at both the frequencies (see Fig. 2). Table 1 gives the details of observing runs with the different radio telescopes and the sensitivities and resolutions that were achieved at various observing frequencies.

For obtaining a spatially resolved spectral index information, we combined GMRT 240- and 621-MHz images for a low frequency spectral index map, and VLA 1.4- and 4.8-GHz images for a high-frequency spectral index map. These are shown in Fig. 6. For this purpose, radio data of MRC 0116+111 were specially processed (if required, by giving suitable tapers in the visibility plane) so as to obtain a uniform angular resolution of 12 arcsec (FWHM beam size) at all the frequencies. When combining the radio images we have included only the pixels with amplitudes ~ 3.5 times above the rms noise, to prevent spurious structures from appearing in the spectral index maps. These cut-offs were given at values 4, 0.5, 0.27 and $0.15 \text{ mJy beam}^{-1}$ on the 240, 621, 1425 and 4860 MHz maps, respectively.

³ The VLA is a facility of the National Radio Astronomy Observatory (NRAO). The NRAO is a facility of the National Science Foundation, operated under cooperative agreement by Associated Universities, Inc.

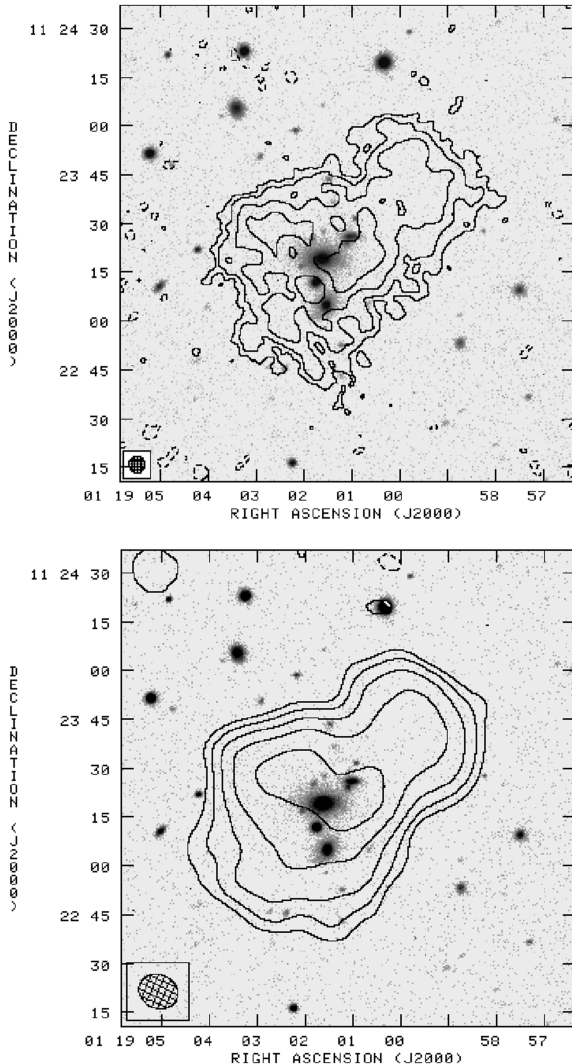


Figure 1. Upper panel: GMRT 1.28-GHz map of MRC 0116+111 shown with contours (levels: $\pm 0.24, 0.48, 0.96, 2, 4$ and 8 mJy beam^{-1} , noise rms $0.08 \text{ mJy beam}^{-1}$, beam: 5 arcsec FWHM circular, plotted inside box) overlayed on IGO *R*-band image. No AGN (radio core) is visible down to $\sim 1 \text{ mJy beam}^{-1}$ flux density limit, and no radio jets or lobes are detectable either. Lower panel: GMRT 240-MHz map shown with contours (levels: $\pm 4, 8, 16, 32, 64$ and $128 \text{ mJy beam}^{-1}$, noise rms $1.35 \text{ mJy beam}^{-1}$, beam: $12.15 \times 10.31 \text{ arcsec}^2$ FWHM at 65.4° position angle (PA), plotted inside box). In the background is shown the IGO *R*-band image of the galaxy cluster.

2.2 Optical imaging and spectroscopic observations

The diffuse radio-halo source MRC 0116+111 was earlier identified by us to be centred on the dominant (cD-like) galaxy of a poor group with three–four members (Gopal-Krishna et al. 2002). Recently, at the position of this radio source a relatively poor galaxy cluster NSCS J011904+112133 was identified by Lopes et al. (2004) in their survey of clusters from Digitized Second Palomar Observatory Sky Survey (DPOSS-II) photographic plates, with a photometric redshift estimate 0.16. However, from our NTT spectroscopy we placed the cluster at a redshift of 0.131 (see Gopal-Krishna et al. 2002 and below). Other than this no other optical or spectroscopic data was found in the literature. We carried out optical broad-band (*B*, *V*, *R*, *I*) imaging observations of the host cluster using the recently commissioned 2-m telescope at the IGO, located

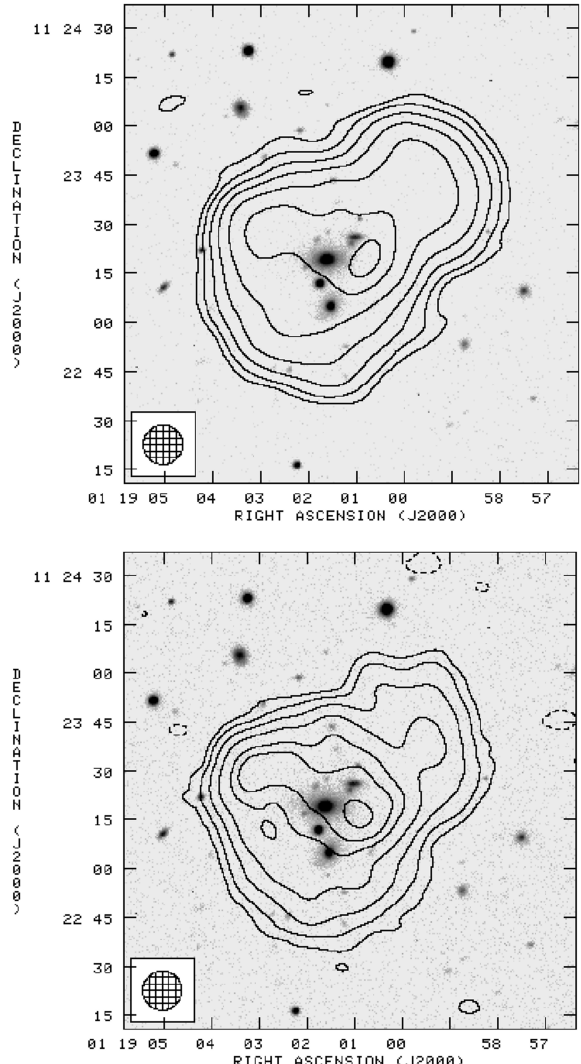


Figure 2. VLA radio maps of MRC 0116+111 overlayed on IGO *R*-band optical image of the galaxy cluster. The upper panel shows *L*-band (1425 MHz) map drawn with contour levels $\pm 0.24, 0.48, 1, 2, 4, 8$ and 12 mJy beam^{-1} and lower panel shows the *C*-band (4860 MHz) map drawn with contour levels $\pm 0.2, 0.4, 0.8, 1.6, 2.2$ and 3 mJy beam^{-1} . The resolution is 12 arcsec for both the images, shown by the FWHM of the beam plotted in the lower left-hand corner.

about 80 km from Pune, India. The observations were taken on the night of 2007 December 31 using the IUCAA Faint Object Spectrograph and Camera (IFOSC) mounted at the Cassegrain focus. IFOSC employs an EEV $2\text{k}\times 2\text{k}$, thinned, back-illuminated CCD with $13.5 \mu\text{m}$ pixels. The spatial sampling scale at the detector is $44 \mu\text{m arcsec}^{-1}$ giving a field of view of about 10.5 arcmin on the side. During observation the seeing conditions were good, but with fair to occasionally poor sky transparency.

We took several frames in each filter with total exposure time sufficient to achieve adequate photometric accuracy. Photometric zero-points and colour transformations were defined by observing Landolt's standard field Rubin 149 (Landolt 1992). The analysis of the CCD frames was done in a standard way using the IRAF software. The *I*-band frames suffered from strong fringing, which could not be completely removed by flat-fielding; therefore, we report only the *B*-, *V*- and *R*-band data in this paper. A composite *B*, *V*, *R* colour image of the host galaxy cluster is shown in Fig. 3. Several

Table 1. Details of GMRT and VLA observations of MRC 0116+111.

Frequency (MHz)	240	621	1280	1425	4860
Telescope	GMRT	GMRT	GMRT	VLA	VLA
Date of observation	2007 December 1	2007 December 1	2007 December 2	1997 June 12	1992 June 22
Flux calibrator	3C 48	3C 48	3C 48	3C 48	3C 48
Bandwidth (MHz)	6	16	16	50	50
Integration time per visibility	16.9 s	16.9 s	16.9 s	10 s	10 s
FWHM synthesized beam	$12.15 \times 10.31 \text{ arcsec}^2$	6 arcsec circular	5 arcsec circular	12 arcsec circular	12 arcsec circular
rms map noise (mJy beam $^{-1}$)	1.35	0.15	0.08	0.08	0.04
Integrated flux density (Jy)	1.15 ± 0.05	0.47 ± 0.01	0.19 ± 0.01	0.140 ± 0.005	0.035 ± 0.005



Figure 3. A B , V , R false-colour composite of the central region of galaxy cluster hosting MRC 0116+111. The region shown is about $8.3 \times 7 \text{ arcmin}^2$ in size and north is on top and east is to the left. This image is made using the IGO 2-m telescope.

elliptical galaxies are visible within the contours of GMRT and VLA radio maps (Figs 1 and 2) with a giant cD-like galaxy of $m_v = 17.69 \text{ mag}$ ($M_v = -21.38 \text{ mag}$) seen in the centre at the position RA = $01^{\text{h}}19^{\text{m}}1.69$, Dec. = $+11^{\circ}23'18.4'$ (J2000).

For spectroscopy we used the ESO/La Silla 3.6-m NTT and EMMI. A $2 \times 10 \text{ min}$ low-resolution slit spectrum (slit width 1.5 arcsec , spectral resolution 3.7\AA) was taken with the grism-3 optics on the EMMI (1991 October) which gave a redshift $z = 0.1316$ for the brightest central cD galaxy (Fig. 4), based on the absorption lines of Na ($\lambda 5893$), Mg b ($\lambda 5169$), H β ($\lambda 4861$), G band ($\lambda 4304$) and the Ca H&K break. A probable weak [O II] ($\lambda 3727$) emission line is visible at the left-most edge of the spectrum, where the signal-to-noise (S/N) ratio is comparatively lower. The second brightest elliptical galaxy $\sim 15 \text{ arcsec}$ south of cD (Fig. 3) was found to have a close redshift $z = 0.1309$, suggesting a group-like environment around the central cD.

3 PHYSICAL PICTURE OF THE RADIO SOURCE

3.1 A twin bubble-like diffuse radio-halo morphology: a ‘quiescent’ radio galaxy?

MRC 0116+111 shows a highly diffuse ‘halo’- or ‘bubble’-like structure which bears close resemblance to the amorphous struc-

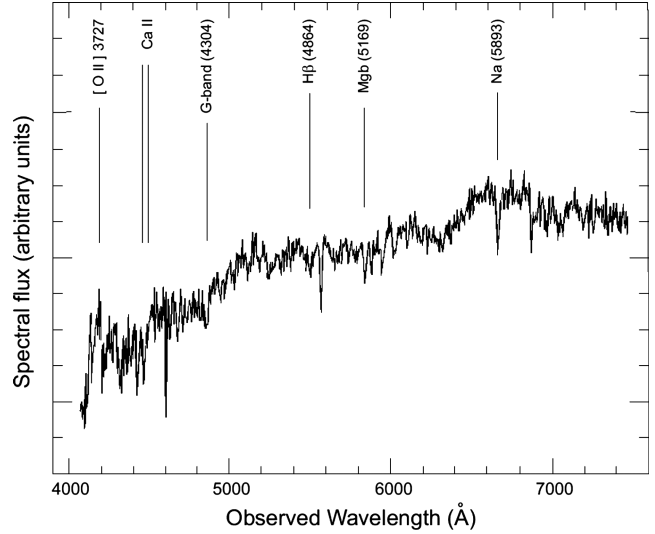


Figure 4. EMMI low-resolution (spectral resolution 3.7\AA) slit spectrum of the central cD galaxy in MRC 0116+111 cluster taken with grism-3 optics on the NTT. The abscissa shows observed wavelengths and ordinate, the spectral flux on an arbitrary scale. The prominent spectral lines are marked along with their rest wavelengths. The spectrum gives a redshift $z = 0.1316$ for this galaxy.

ture of so-called ‘radio minihaloes’ (see Section 1 and Ferrari et al. 2008). The physical size, radio spectral index and morphology of MRC 0116+111 are broadly consistent with the properties of a cluster radio minihalo. In Table 3 we compare the physical properties of MRC 0116+111 with a few other well-known radio minihaloes, including the well-known radio galaxy Virgo A (M87). We note that the radio luminosity of MRC 0116+111 at 1.4 GHz , $L_{1.4 \text{ GHz}} = 4.57 \times 10^{24} \text{ W Hz}^{-1}$, is quite large, comparable to the luminous radio haloes in Perseus and A2390 clusters. Furthermore, its bolometric radio luminosity (over 10 MHz – 10 GHz range), $L_{\text{radio}} = 3.64 \times 10^{34} \text{ W}$, close to the divide between Fanaroff–Riley I (FR-I) and Fanaroff–Riley II (FR-II) class radio sources, would place it amongst the most luminous radio haloes known.

GMRT 621-MHz radio map of MRC 0116+111 (Fig. 7) and its other radio maps (Figs 1 and 2) clearly show that on larger scales ($\sim 100 \text{ kpc}$) the radio-halo emission comprises of two diffuse ‘lobe’-like structures surrounding the central group of galaxies, which we suggest are actually a pair of giant, radio emitting plasma bubbles, filled with relativistic particles (cosmic rays) and magnetic field. In Fig. 7 the dotted lines delineate this pair of radio bubbles, having the projected dimensions $\sim 27.5 \times 17.5 \text{ arcsec}^2$ ($= 64.4 \times 41 \text{ kpc}^2$) – the semimajor and minor axes of ellipse for the smaller elliptical north-west bubble, and $\sim 35 \text{ arcsec}$ ($= 82 \text{ kpc}$) radius for the larger spherical bubble to south-east of the cluster centre.

The total spatial extent of radio emission is ~ 240 kpc which apparently surrounds the dominant brightest cD-like elliptical galaxy of the cluster (Fig. 3). However, based on the detection sensitivities achieved in our present GMRT and VLA observations (see Table 1), there is no strong evidence that the extended radio emission emanates from this or any other galaxy enclosed within the radio contours. The highest resolution GMRT 1.28-GHz map (Fig. 1) and other radio maps have not detected a compact active radio nucleus (AGN) and radio jets directly feeding into the 100-kpc scale twin plasma lobes/bubbles of MRC 0116+111. In this respect MRC 0116+111 is very unusual and it differs from other well-known minihaloes, including canonical M87 and Perseus A (Pedlar et al. 1990; Owen, Eilek & Kassim 2000; Cassano, Gitti & Brunetti 2008; Ferrari et al. 2008), which have detectable powerful AGN cores and jets. The high-resolution GMRT 1.28-GHz image of MRC 0116+111 also does not show any other compact AGN-related background sources blended with the radio-halo emission, which clearly rules out its origin from such a contamination (Fig. 1).

Therefore, this suggests to us a physical picture in which the relativistic particles and magnetic fields of MRC 0116+111 halo were initially seeded by a pair of radio jets originating in AGN activity in the past, most likely from the nuclear SMBH of the central cD galaxy, as revealed by the pair of plasma bubbles straddling this galaxy. However, at present MRC 0116+111 resembles a quiescent or ‘fossil’ source – in the sense that its twin extended lobes/bubbles of radio plasma not energized by active jets from an AGN – as observed in classical radio galaxies. This suggests that the SMBH embedded in the nucleus of the cD galaxy, which was once active, probably has turned-off its radio jets sometimes back in the past. Only a handful of such ‘fossil’ or ‘dying’ radio galaxies are known so far, which are more easily detected at low radio frequencies due to their very steep spectra (e.g. Jamrozy et al. 2004; Parma et al. 2007). It is possible that we have caught the central massive black hole, which created MRC 0116+111, during a low or even quiescent state of its activity cycle. If the heat input into the ICM by these expanding radio bubbles is large enough to significantly offset the cooling loss, the flow of accreting matter on to the SMBH may stop, thus starving the ‘central engine’ of its fuel. So we expect that this radio bubble-fed energy exchange should give rise to an episodic triggering of the AGN itself, establishing a self-regulated activity pattern between cooling flow and AGN activity. We point out that this cyclic process, even if in operation, does not imply that some form of *in situ* re-acceleration of particles in shocks or turbulence does not take place in the central cooling core and the extended lobes of MRC 0116+111 – a scenario, in fact supported by both the integrated radio spectrum and the spectral index maps discussed below.

3.2 Possible location of MRC 0116+111 in a low-mass poor-cluster/group environment

According to our present understanding of the origin and evolution of minihaloes, their diffuse, steep-spectrum halo or bubble-like morphology results from strong interaction of radio jets with the surrounding dense and cool gaseous medium of the cluster core. At present there are no available good X-ray data for this system and therefore we lack information about the physical state of ICM in the core of cluster hosting MRC 0116+111. Such data are required for quantifying accurately the energy input rate by the AGN jets into the plasma bubbles of minihalo as well as their dynamics and interaction with the ICM. The X-ray luminosity is also a good indicator of the optical richness and mass of the host system. We find that

the miniradio halo MRC 0116+111 is located in an underexposed region of *ROSAT* All Sky Survey (RASS), which only allows us to determine an upper limit of $<1.4 \times 10^{43}$ erg s $^{-1}$ for its X-ray luminosity in 0.5–2 keV band.

However, based on the mass–X-ray luminosity relation, the upper limit on the X-ray luminosity of MRC 0116+111 translates to an upper limit for the gravitational mass of its host cluster/group of about $10^{14} M_{\odot}$ (e.g. Reiprich & Böhringer 2002; Stanek et al. 2006). This suggests that MRC 0116+111 is possibly located at the centre of a poor-cluster or a rich-group environment, which is also corroborated by the (photographically estimated) low galaxy density reported by Lopes et al. (2004) for the galaxy cluster NSCS J011904+112133, which hosts MRC 0116+111. This is a rather surprising result which makes MRC 0116+111 special because in general, all other known miniradio haloes are found within X-ray bright cooling cores (Table 3) with X-ray luminosity $\gtrsim 10^{44}$ erg s $^{-1}$, and some of the most powerful systems may have luminosity $\sim 10^{45}$ erg s $^{-1}$.

3.3 Spectral index plot: the ‘break’ frequency and radiative ageing analysis

As these 100-kpc scale giant radio-emitting magnetized bubbles in MRC 0116+111 suggest their origin in intermittent AGN activity, we can estimate the time-scale of such outbursts from the shape of total radio spectrum and the spectral index maps. Spectral index represents a powerful tool to study the properties of the relativistic electrons and the magnetic field in which they radiate, and to investigate the connection between the electron energy and the ICM. From our multifrequency radio imaging and published data, we have derived the integrated spectrum (Fig. 5) and spatially resolved spectral index maps (Fig. 6). Low-frequency (~ 100 –400 MHz) spectra are important to determine the slope of electron energy distribution and preserve a record of past AGN activity, while the high-frequency spectra (~ 1 –10 GHz) give information on the diffusion and ageing of relativistic particles, and any particle (re)acceleration mechanism that may be in operation.

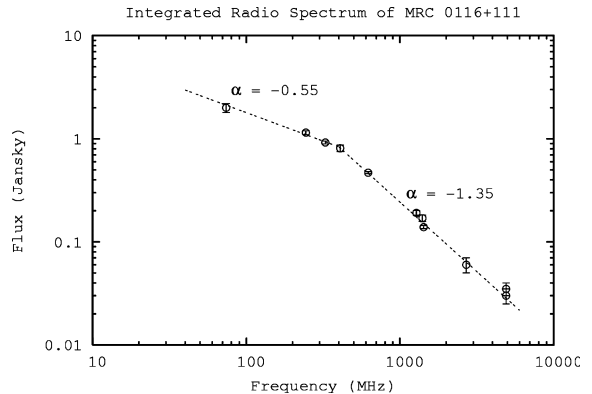


Figure 5. The integrated radio spectrum of MRC 0116+111 between 74 MHz and 4.9 GHz. Piecewise linear least-squares fit to the data points shows a sudden spectral steepening beyond the ‘break’ frequency $\nu_{\text{br}} \approx 400$ MHz. The low-frequency spectral index is $\alpha_1 = -0.55 (\pm 0.05)$, and the high-frequency spectral index is $\alpha_h = -1.35 (\pm 0.06)$. The GMRT and VLA observed flux density values are listed in Table 1. Other data points are taken from literature as follows: 74 MHz (VLSS: Cohen et al. 2007), 327 MHz (Gopal-Krishna et al. 2002), 408 MHz (Molonglo: Large et al. 1981), 1400 MHz (NVSS: Condon et al. 1998), 2700 MHz (Effelsberg: Gopal-Krishna et al. 2002) and 4.8 GHz (GreenBank: Becker, White & Edwards 1991).

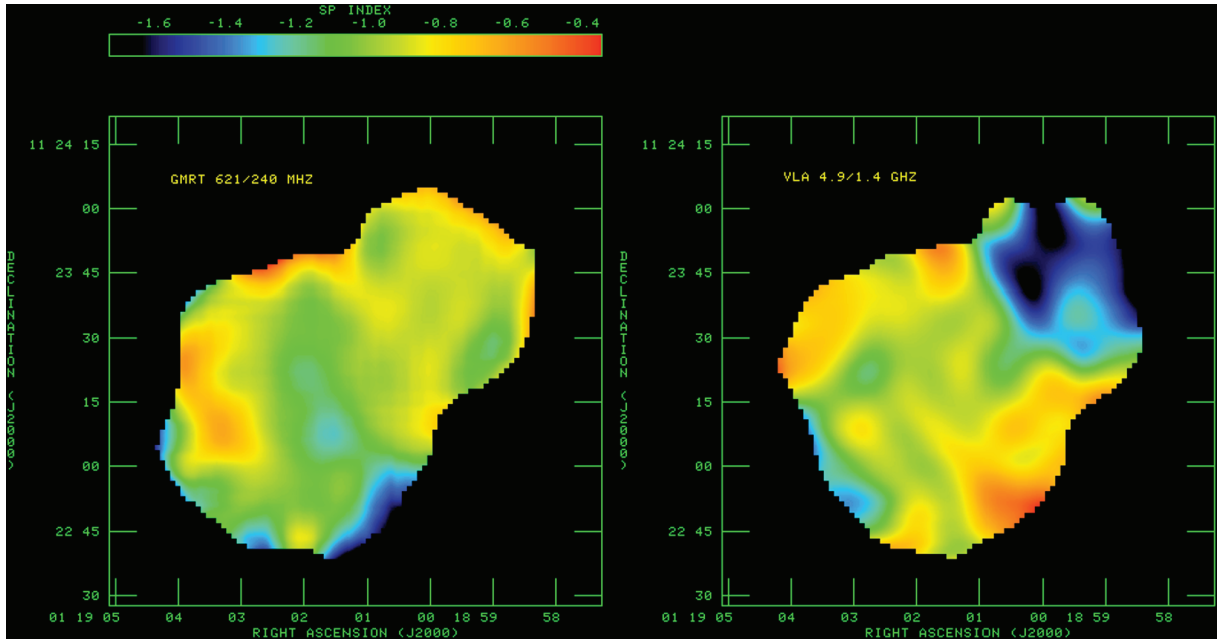


Figure 6. Low- and high-frequency spectral index maps of MRC 0116+111 obtained by combining the GMRT radio maps at 240 and 621 MHz (left-hand panel) and VLA maps at 1425 and 4860 MHz (right-hand panel). Both pairs of maps have the matched resolution of 12 arcsec (FWHM). To prevent spurious structures from appearing, only pixels above ~ 3.5 times the rms noise level were included by giving cut-offs at values 4, 0.5, 0.27 and 0.15 mJy beam $^{-1}$ at 240, 621, 1425 and 4860 MHz, respectively. The colour bar shows the spectral index values. A significant spectral steepening (mean $\alpha = -1.6$) for the north-western bubble at high frequency can be clearly seen.

The integrated radio spectrum between 74 MHz and 4.9 GHz frequencies shows a strong downward curvature (Fig. 5). Piecewise linear least-squares fit shows an onset of spectral steepening beyond the critical (also known as ‘break’) frequency $\nu_c \sim 400$ MHz. The low-frequency spectral index is $\alpha_l = -0.55(\pm 0.05)$, while the high-frequency spectral index attains a slope $\alpha_h = -1.35(\pm 0.06)$. The steep spectral index of MRC 0116+111 is consistent with the miniradio-halo morphology which usually have steep radio spectrum ($\alpha < -1$; Ferrari et al. 2008). If the relativistic electrons are all injected in a single energetic outburst with a power-law energy distribution, $N(E) dE = N_0 E^{-p} dE$ (here N_0 is amplitude and $N(E) dE$ the differential number density within energy E to $E + dE$, and p the power-law index), subject to strong radiation losses in synchrotron and inverse Compton processes, the radio spectrum would cut-off rapidly to zero for frequencies above a critical frequency $\nu > \nu_c$, which shifts to lower values with time. In contrast, if episodic injection of fresh particles, or re-acceleration of existing particles takes place in the source, only a spectral steepening by ~ 0.5 beyond the critical frequency occurs. In MRC 0116+111 beyond the critical frequency ν_c the radio spectrum steepens due to radiative losses, but no rapid cut-off is seen (Fig. 5), which suggests an episodic or multiple particle injection process rather than a single energetic outburst event.

The spectral age t_{sp} derived from the synchrotron radio spectrum is given by (Slee et al. 2001)

$$t_{sp} = 1.59 \times 10^9 \frac{B^{0.5}}{(B^2 + B_{CMB}^2) [\nu_c(1+z)]^{0.5}} \text{ yr}, \quad (1)$$

where the magnetic field B is in μG , the critical frequency ν_c in GHz and $B_{CMB} = 3.2(1+z)^2 \mu\text{G}$ is the equivalent ‘magnetic field’ of the cosmic microwave background (CMB) radiation at redshift z . This formula assumes isotropic pitch-angle distribution, no expansion losses and a uniform magnetic field which remained unchanged over the radiative age. For $\nu_c = 400$ MHz and magnetic field range

$B = 1\text{--}10 \mu\text{G}$, the electron spectral age is $t_{sp} = (1.33\text{--}0.64) \times 10^8$ yr, which can be taken as the elapsed time since last injection of relativistic particles in the source. The largest uncertainty in estimation of spectral age is imposed by magnetic field B . Presently we do not have X-ray observation of this source, but from the observed miniradio-halo morphology, it is likely that MRC 0116+111, in common with other known miniradio haloes, would be located at the centre of a cluster cooling core, which in general have stronger ICM magnetic fields of order $B = 10\text{--}30 \mu\text{G}$ compared to non-cooling-core clusters (Soker & Sarazin 1990; Govoni & Feretti 2004). Therefore, $t_{sp} \sim \text{few} \times 10^7$ yr is a more likely (globally averaged) radiative time-scale for MRC 0116+111.

The injection of relativistic particles in the medium can take place via an episodic on-off mechanism of the radio jets driven by the central AGN (even though no radio core or jets are visible down to ~ 1 mJy beam $^{-1}$ level), or via a Fermi-type shock/turbulent re-acceleration mechanism. The requirement is that cooling time $t_{cool} \approx t_{sp}$ should be longer than either the time interval t_{int} between two successive nuclear outburst, or the acceleration time-scale t_{acc} for electrons emitting at frequencies $\nu \gtrsim \nu_c$, i.e. $t_{sp} > t_{int}$ or $t_{sp} > t_{acc}$. It should be added that a lack of spectral cut-off up to the highest observed frequency $\nu = 4.86$ GHz, where electron cooling time-scale $t_{cool} \approx 1.8 \times 10^7$ yr ($B = 10 \mu\text{G}$), puts a severe constraint on the acceleration time-scale, which should be shorter than this, irrespective of the acceleration mechanism.

3.4 Spectral index maps: particle re-acceleration and a buoyantly rising plasma bubble?

Here we present the spatially resolved spectral index maps which reveal interesting details of the radiative energy loss, particle re-acceleration processes and bubble dynamics in this radio source. The spectral slope of radiation emitted from different parts of the source is indicative of radiative ageing (or lack of it) of emitting

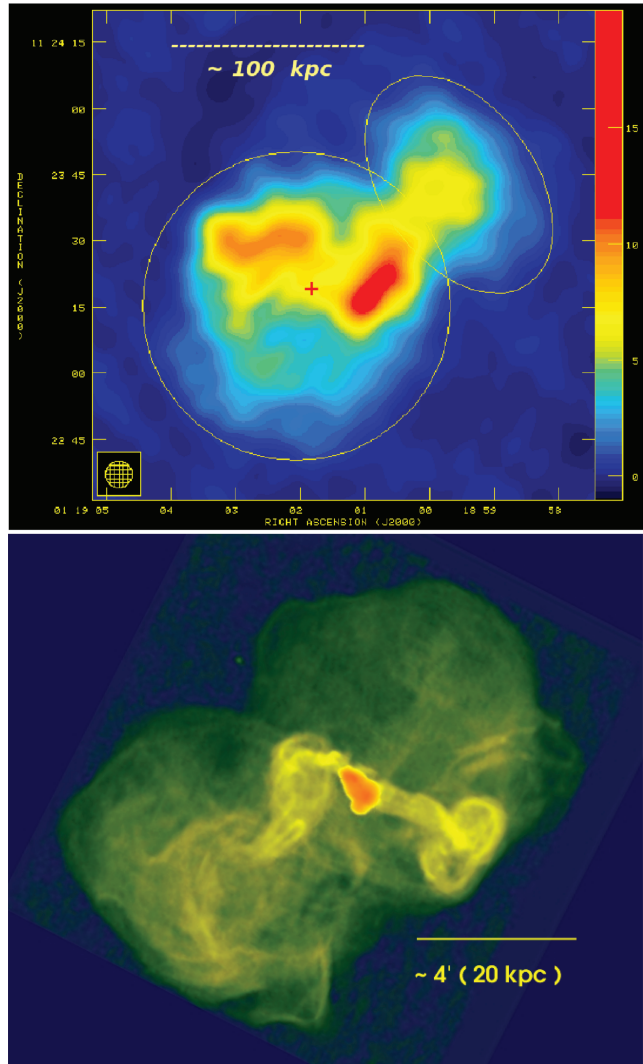


Figure 7. Upper figure: GMRT 621-MHz false-colour image of MRC 0116+111 (beam: 6 arcsec FWHM circular, plotted inside the box) showing the twin bubble-like diffuse radio structure. The colour bar shows surface brightness in mJy beam^{-1} units, and position of brightest central galaxy (cD) is shown by a ‘+’ symbol. The dotted lines delineate the two radio bubbles having projected dimensions $\sim 27.5 \times 17.5 \text{ arcsec}^2$ (semimajor and minor axes of ellipse) for the smaller elliptical north-west bubble and $\sim 35 \text{ arcsec}$ (circular radius) for the spherical larger bubble south-east of the cluster centre. Lower figure: the VLA 90-cm radio image of M87, the dominant central radio galaxy in the Virgo cluster (Owen et al. 2000). The original map has been reflected and rotated for a better comparison with the MRC 0116+111 radio map (reproduced by permission of the AAS).

particles. The low- and high-frequency spectral index maps are presented in Fig. 6. These maps show that between 240 and 621 MHz the spectral index distribution is fairly uniform with no strong steepening or gradients across the source ($\alpha_{\text{mean}} = -1.02 \pm 0.17$ for south-western bubble and $\alpha_{\text{mean}} = -0.95 \pm 0.10$ for the north-eastern bubble, which are marked in Fig. 7), implying a lack of strong radiative losses between these frequencies (Fig. 6, left-hand panel). However, the high-frequency spectral index map between 1.4 and 4.8 GHz presents a strikingly different picture (Fig. 6, right-hand panel). On this map, while the south-eastern bubble still has the same average spectral index value around -1 ($\alpha_{\text{mean}} = -1.06 \pm 0.15$) – implying a straight synchrotron spectrum between low and

high radio frequencies – the north-west bubble, in contrast has developed an extremely steep spectrum ($\alpha_{\text{mean}} = -1.6 \pm 0.20$), most likely due to strong radiative energy losses in this part of the source.

Such a situation might be explained if we assume that the north-western bubble showing the very steep spectrum is buoyantly rising away and then detaching itself from a centrally located mechanism of energy injection, while this source or mechanism is still active and possibly injecting relativistic particles into the relatively flatter spectrum south-eastern bubble. One possibility is AGN related activity connected to a supermassive nuclear black hole, which is suggested by the large bolometric radio luminosity of MRC 0116+111 ($L_{\text{radio}} = 3.64 \times 10^{34} \text{ W}$, see Table 2), though we fail to detect a nuclear core or active jets (Fig. 1). It is plausible that these bubbles are tracers of a previous cycle of AGN activity. Thus, a possible scenario is that these bubbles were inflated by the pressure of radio jets in a previous very energetic episode of AGN activity which has either stopped now or has become too feeble to be detectable. During the later stages of evolution the dynamics of the remnants of the radio jets will be dominated by buoyancy forces and drag (e.g. Gull & Northover 1973; Churazov et al. 2001), as they interact with the cluster atmosphere in the inner core region. Our detection of a possibly buoyantly rising plasma bubble is also significant from theoretical point of view, as one of the most appealing and widely applied models in literature for heating of ICM involves buoyant gas bubbles, inflated by AGN source, that subsequently rise through the ICM and heat it up (e.g. Böhringer et al. 2002; Bruggen & Kaiser 2002; Bruggen et al. 2002; Churazov et al. 2002; Cattaneo & Teyssier 2007; Ruszkowski et al. 2008). We further discuss the physics of these radio bubbles in the sections below.

3.5 Remarkable morphological similarity with the twin radio bubbles of M87 (Virgo A)

Our radio observations presented above clearly show that MRC 0116+111 is a striking example of a radio-halo source consisting of twin plasma bubbles, possibly inflated in a previous episode of AGN outburst from a SMBH. We wish to point out that, in this respect, it closely resembles the radio emitting bubbles observed around M87, the dominant central radio galaxy of the Virgo cluster (Owen et al. 2000), 3C 84, the central cD in Perseus cluster (Pedlar et al. 1990), and 3C 218, the central radio source in Hydra cluster (McNamara et al. 2000; Wise et al. 2007). However, as we have pointed out above, a notable major difference is that while these (and other cluster centre radio minihaloes, see Table 3) exhibit the central galaxy’s active nucleus (central core) and visible jet structure, MRC 0116+111 in contrast is probably a quiescent source, lacking an active AGN and ongoing radio jet activity. Therefore, MRC 0116+111 is quite unusual and presents a unique opportunity to understand the dynamical evolution and impact of radio jet inflated plasma bubbles on the ICM, when the central AGN activity approaches cessation (probably when the fuel supply to the SMBH is exhausted), or when the non-thermal bubbles start rising buoyantly and detaching themselves from the flow.

For a closer comparison, in Fig. 7 we show the 621-MHz radio image of MRC 0116+111 and a deep VLA 90-cm image of M87 published by Owen et al. (2000) (the original image has been reflected and rotated for better comparison with MRC 0116+111). The morphological similarity between the two radio sources is striking. Owen et al. (2000) found that in M87, beyond the well-known inner-jet and lobe region (which appears as the 2-kpc scale red-orange patch near the centre of M87, Fig. 7), there is diffuse outer structure extending up to ~ 40 kpc from the nucleus, which is known

Table 2. Observed and calculated parameters.

Spectroscopic redshift (central cD galaxy)	0.1316
Apparent magnitudes ^a (central cD galaxy)	$m_B = 18.79, m_V = 17.69, m_R = 16.69$
621-MHz radio luminosity ($L_{621\text{MHz}}$)	$1.21 \times 10^{25} \text{ W Hz}^{-1}$
1400-MHz radio luminosity ($L_{1.4\text{GHz}}$)	$4.57 \times 10^{24} \text{ W Hz}^{-1}$
Bolometric radio luminosity (L_{radio}) (over 10 MHz–10 GHz range)	$3.64 \times 10^{34} \text{ W}$
‘Break’ frequency in spectrum	~400 MHz
Elliptical north-west bubble dimension (projected semimajor and minor axes)	$\sim 27.5 \times 17.5 \text{ arcsec}^2 (= 64.4 \times 41 \text{ kpc}^2)$
Circular south-east bubble dimension (projected circular radius)	~35 arcsec (= 82 kpc)

^aCorrected for galactic extinction (NASA Extragalactic Database).

Table 3. Comparison of MRC 0116+111 with other known miniradio haloes^a. Column 1: cluster name; column 2: cluster redshift; column 3: log X-ray luminosity of the cluster in energy range 0.1–2.4 keV; column 4: log 1.4-GHz radio luminosity; column 5: log radio halo radius in kpc.

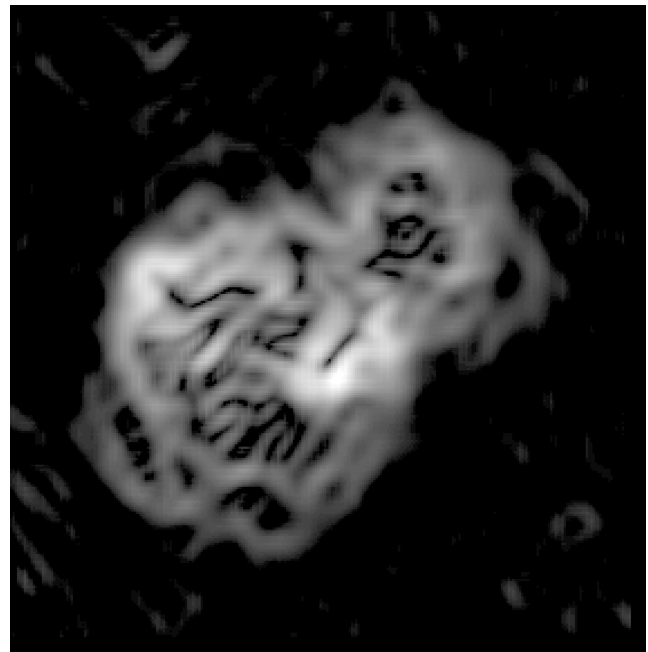
Name	Redshift	Log L_X (erg s ⁻¹)	Log $L_{1.4\text{GHz}}$ (W Hz ⁻¹)	Log R_H (kpc)
Perseus	0.018	44.82	24.27	2.12
A2390	0.228	45.13	24.99	2.26
A2626	0.060	44.03	23.36	1.85
RX J1347.5–1145	0.451	45.65	25.28	2.41
Z7160	0.258	44.93	24.34	2.24
RBS 797	0.350	45.31	24.63	2.01
M87	0.004	43.90	24.72	1.60
MRC 0116+111	0.131	<43.15 ^b	24.66	2.08

^aData from Birzan et al. (2008) and Cassano et al. (2008).

^bUpper limit estimated by us from RASS data in 0.5–2 keV band.

to host a central SMBH with a mass of $3.2 \times 10^9 M_\odot$ (Harms et al. 1994). Two large-scale collimated flows emerge from the inner-jet region, one directed north-eastward and the other oppositely directed to south-westward (orientations refer to the rotated image). Particularly intriguing is a well-defined pair of edge-brightened, ‘ear-shaped’ torus-like structure at the end of south-west flow, which is reminiscent of a subsonic vortex ring. The north-eastern flow develops a gradual but well-defined S-shaped southward twist, starting only a few kiloparsecs beyond the inner lobes. Finally, both flows are embedded in a giant diffuse radio structure that might be described as two overlapping ‘bubbles’, each extending about 40 kpc from the nucleus. After reaching the halo, the flows gradually disperse, particularly the north-eastward flow, and appear to be filling the entire halo with radio-loud, filamented plasma.

We observe similar flow pattern in the central region of MRC 0116+111, despite the limited spatial resolution available. As shown in Fig. 7, an edge brightened torus-like ‘mushroom’ structure is observed about 40 kpc west of centre of the larger south-eastern bubble, which might well be analogous to the peculiar ‘ear-shaped’ vortex structure of M87. Here the flow pattern sharply turns northward and appear to be flowing into the smaller radio bubble to the north-west. We observe an S-shaped flow pattern to north-east of centre, which further bends to south, and clearly resembles the filamentary structure found in the southern bubble of M87. In order to better visualize a possible filamentary structure of synchrotron plasma bubbles, we have digitally image processed the 621-MHz map of MRC 0116+111 with the AIPS task NINER for a gradient filter operation, which enhances sharp intensity gradients and suppresses

**Figure 8.** An image processed view of GMRT 621-MHz image of MRC 0116+111 shown in Fig. 7. We have used the ‘Sobel’ gradient filter operation as implemented in AIPS task NINER to enhance sharp intensity gradients and suppress diffuse emission. Highly intricate filamentary structures of radio emitting plasma interior to the radio halo can be seen.

diffuse emission. The resulting image reveals (Fig. 8), akin to M87, a highly complex filamentary structure of plasma embedded in the radio halo. However, with the available angular resolution (6 arcsec FWHM beam size) far less details are visible in MRC 0116+111 as compared to M87, mainly because it is much farther away from us than M87. Of course, as mentioned above, in our radio observations of MRC 0116+111 we find no evidence for a strong AGN core, inner jets and lobe structures, which clearly are present in M87. One feature which makes the case of MRC 0116+111 especially interesting is that the inner plasma outflow structures in both these radio sources are surrounded by a pair of diffuse radio emitting ‘bubble’-shaped giant lobes. We note that large misalignment seen in these two cases, between the inner outflow structure and the surrounding minihalo may in fact be fairly common, exhibited by several other minihaloes. Examples include A2626 and the prototypical minihalo in Perseus A (Pedlar et al. 1990; Gitti et al. 2004). All this hints towards a common mechanism, namely the radio jets

from AGN, strongly interacting with the confining environment of a cooling core, forming an amorphous minihalo structure.

Moreover, it is also interesting to note that although MRC 0116+111 closely resembles M87 in its radio morphology, at ~ 240 kpc its total linear size is about three times larger than M87, which spans a scale of just ~ 80 kpc (Owen et al. 2000 and Table 2). The bolometric radio luminosity of both is about the same; $L_{\text{radio}} = 3.64 \times 10^{34}$ W for MRC 0116+111 and $L_{\text{radio}} = 3.6 \times 10^{34}$ W for M87 (Birzan et al. 2008). This in turn implies that the average volume emissivity of MRC 0116+111 is almost 30 times smaller than that of M87.

4 DISCUSSION

The similarity of large-scale radio plasma outflow structures observed in MRC 0116+111 and M87 suggests that both sources might have originated in, and their evolution governed by, similar physical process and conditions prevailing in the central regions of their host clusters. The origin of extremely complex diffuse radio structures observed in the outer radio bubbles of M87 and other similar radio minihalo objects is not yet fully understood. From hydrodynamic simulation Churazov et al. (2001) suggested that the twin bubbles in M87 are buoyant bubbles of cosmic rays and magnetic fields, inflated by jets launched during an earlier nuclear active phase of the central galaxy, which rise through the cooling gas at roughly half its sound speed. On the contrary, Owen et al. (2000) favour a scenario in which the radio halo of M87 is not simply a relic of previous episode of AGN activity but presently it is ‘alive’, such that it is being supplied with relativistic particles coming from the central AGN and the innermost radio jets. As revealed in our radio observations, non-detection of a strong AGN core, inner-jets and lobe/hotspot structure in MRC 0116+111, coupled with the detection of a ~ 100 -kpc scale radio bubble of very steep spectrum north-west of the cluster centre supports the ‘buoyantly rising bubble’ model of Churazov et al. (2001). The flattened ‘mushroom’ shape of this plasma bubble indeed resembles a rapidly rising vortex ring (Fig. 7), into which an initially spherical bubble will naturally transform due to viscosity and drag forces (Churazov et al. 2001; Bruggen et al. 2002). The present quiescent/low state of the central engine suggests an on-off activity cycle of the SMBH. That such activity is intermittent and the central AGN is periodically rejuvenated is suggested by the high incidence of bubbles found in cluster cores that require heating to counter balance the cooling flow (Dunn & Fabian 2006), and by the train of ghost bubbles and pressure ripples observed in Perseus and Hydra clusters (Sanders & Fabian 2007; Wise et al. 2007). Furthermore, the distant cooling core cluster RBS 797 shows an inner radio jet pair oriented perpendicular to that of the extended radio-halo structure and X-ray cavities, suggesting restarting activity of AGN (Gitti, Feretti & Schindler 2006).

An important question raised by our observations is: what energizes the relativistic particles in the central region of MRC 0116+111, which apparently counter balances the strong radiation losses and prevents severe steepening of radio spectrum? The properties and physical processes governing the origin and evolution of radio minihalo sources are poorly understood due to their rather small numbers known till now (less than 10). Based on a sample of five–six minihaloes, Gitti et al. (2004) have reported a positive correlation between the radio power of minihalo and the cooling flow radiative power. From this, and because of their estimate of the lifetimes of the radiating electrons falling considerably short of the diffusion time-scale, they have argued that in minihaloes

the cooling flow (through the compressional work done on the ICM and amplification of frozen-in magnetic field) energizes the particle acceleration process through magnetoplasma turbulence acting on relic electron population probably left behind by the past episodes of AGN activity. This suggests a direct connection between cooling flows and radio minihaloes. With a detailed spectral fitting of the radio spectrum and emission profile with the parameters derived from the turbulent re-acceleration model, it will be possible to test the viability of this mechanism for the present source.

An alternative proposal is that the radiating electrons in the minihaloes are of secondary hadronic origin (via the pion decay route), created in proton–proton ($P_{\text{CR}} - P_{\text{th}}$) collisions (Pfrommer & Ensslin 2004) of high energy cosmic ray (CR) protons (P_{CR}) with target thermal protons (P_{th}). The CR protons may originate in several ways: in large-scale structure formation shock waves (Colafrancesco & Blasi 1998; Loeb & Waxman 2000; Ryu et al. 2003; Bagchi et al. 2006), or through supernovae and galactic winds from central galaxies (Völk, Aharonian & Breitschwerdt 1996) or via powerful AGNs injecting CRs into the ICM (Ensslin et al. 1997; Aharonian 2002; Pfrommer & Ensslin 2004). A clear signature of this process is emission of γ -ray photons of broad energy range $E_{\gamma} \sim 100$ MeV–10 TeV, accompanying decay of neutral pions (π^0) produced in inelastic proton–proton collisions. Therefore, the hadronic model should be testable in near future with sensitive γ -ray observations. Recently, Hinton, Domainko & Pope (2007) applied the hadronic CR injection model to three galaxy clusters (Hydra A, MS 0735.6+7421 and Hercules A) harbouring the most energetic AGN outbursts known (with mechanical energy input of AGN at least 10^{61} erg). They concluded that the γ -ray observability of these objects is at the threshold of detectability with current (FERMI, HESS), and near future γ -ray instruments, if the observed radio bubbles are dominated by the pressure of relativistic particles. Therefore, such observations are obviously of great importance for deciphering the connection between the energetic CR and thermal energy content of clusters harbouring the radio haloes.

We have estimated the volume of the two radio bubbles from their projected dimensions on the GMRT 621-MHz image (Fig. 7; Table 2). The volumes are $V_1 = 4/3(\pi r_1^3) = 6.78 \times 10^{70}$ cm³ for the spherical south-west bubble of radius $r_1 = 82$ kpc, and $V_2 = 4/3(\pi a^2 b) = 2.08 \times 10^{70}$ cm³ for the ellipsoidal north-west bubble (we model it as an oblate spheroid with semimajor axis $a = 64.4$ kpc and semiminor axis $b = 41$ kpc). The volume $V = V_1 + V_2 = 8.86 \times 10^{70}$ cm³ is the total volume occupied by relativistic particles and magnetic fields, which we assume to be mainly supplied by the radio jets and not produced in local shocks. The linear dimension of the present radio bubbles is $l_{\text{bubble}} \sim 100$ kpc, which is much larger compared to the typical dimensions of X-ray cavities ($l_{\text{cavity}} \sim 1$ –20 kpc; Birzan et al. 2004), and they are comparable to the ~ 100 –200 kpc size supercavities found in MS 0735.6+7421 and Hydra clusters (McNamara et al. 2000, 2005; Wise et al. 2007).

The large radio luminosity and linear size of the radio bubbles in MRC 0116+111 suggest that radio jets from AGN must have done large amount of mechanical work (pdV) in inflating them against the external pressure of thermal ICM gas, as well as injected enormous non-thermal plasma energy (magnetic field and relativistic particles), which has remained stored inside the bubbles, as they rose buoyantly under pressure equilibrium with the external medium. Future X-ray observations of MRC 0116+111 would reveal if the relativistic fluid filling these bubbles has pushed aside the thermal gas, excavating giant cavities in the X-ray emitting ICM. We have detected a buoyantly rising radio bubble ~ 100 kpc from the centre of radio halo (Fig. 6). Such bubbles result from

displacement of the thermal gas, which creates a low-density bubble maintained in pressure balance with the surrounding medium and rising subsonically. These non-thermal plasma bubbles associated with X-ray cavities found in the ICM of clusters are turning out to be excellent ‘calorimeters’ for gauging the total mechanical power of radio jets from AGNs. Such measurements are extremely useful as they not only preserve the past record of enormous outbursts of the central SMBH, but are also independent of the radio properties of the jets (i.e. their present radiative output and magnetic field strength), allowing a good estimate of energy injected into the surrounding thermal plasma for heating it (e.g. Churazov et al. 2002; Birzan et al. 2004, 2008).

A thermodynamical measure of the total energy required to slowly inflate a hot cavity/bubble in ICM is given by its enthalpy, $H_{\text{cav}} = [\gamma/(\gamma - 1)]pV$, where γ is ratio of specific heats of the gas inside the cavity, p is the pressure of external medium and V is the volume of the cavity (Churazov et al. 2002; Birzan et al. 2004). For a radio jet inflated non-thermal bubble, which has completely displaced the thermal medium, $\gamma = 4/3$ and $H_{\text{cav}} = 4pV$. The external pressure is $p = \rho_{\text{ICM}}kT/(\mu m_{\text{H}})$ (where ρ_{ICM} is the density of ICM, T is the gas temperature, $\mu = 0.6$ the mean molecular weight and m_{H} is mass of the hydrogen atom), which is presently not known for MRC 0116+111. We can obtain an order of magnitude estimate for H_{cav} if we take fiducial values, $\rho_{\text{ICM}} = 1.67 \times 10^{-26} \text{ gm cm}^{-3}$ (for a proton number density of 10^{-2} cm^{-3}) and $T = 2.32 \times 10^7 \text{ K}$ (2 keV), which are typical of the gaseous environment around a miniradio-halo source like M87 or Perseus A at the centre of a cooling core (Ghizzardi, Molendi & Pizzolato 2004). This gives a pressure $p = 5.3 \times 10^{-11} \text{ dynes cm}^{-2}$ and an enthalpy $H_{\text{cav}} = 2.06 \times 10^{60} V_{70} \text{ erg}$ for a cavity volume $V_{70} = V/(70 \text{ cm}^3)$.

Using the measured volumes of the two radio bubbles in MRC 0116+111 (see above), we estimate an enthalpy $H_1 = 1.39 \times 10^{61} \text{ erg}$ for the south-east bubble, and $H_2 = 4.28 \times 10^{60} \text{ erg}$ for the north-west ‘buoyant’ bubble, resulting in total enthalpy $H_{1+2} = 1.82 \times 10^{61} \text{ erg}$. We require X-ray data to estimate the external ICM pressure around the bubbles; but conservatively, even if this is 1/10 of the value assumed above, we get a total enthalpy $H_{1+2} \sim 10^{60} \text{ erg}$ which is still quite large, but for an order-of-magnitude consistent with the large radio luminosity and huge volumes of these bubbles. The energy injection rate (mechanical luminosity) of radio jets, that inflated the radio bubbles, is $L_j \approx H_{1+2}/t_j$, where t_j is the time interval for which jets were active out of the total activity cycle time t_d of the AGN. Various lines of evidence show that for radio galaxies typically, $t_d \approx \text{few} \times 10^8 \text{ yr}$, and assuming $t_j \sim \text{few} \times 10^7 \text{ yr}$ with $H_{1+2} \sim 10^{60} \text{ erg}$ would lead to $L_j \sim \text{few} \times 10^{44} \text{ erg s}^{-1}$. Birzan et al. (2008) derived an empirical relation (with considerable scatter): $\log L_{\text{cav}} = (0.35 \pm 0.07) \log L_{1.4 \text{ GHz}} + (1.85 \pm 0.17)$, connecting the estimated mechanical jet luminosities of radio AGNs ($L_j = L_{\text{cav}}$) that have associated X-ray cavities, and their 1.4 GHz monochromatic radio luminosities. In this relation $L_{1.4 \text{ GHz}}$ is in units of $10^{24} \text{ W Hz}^{-1}$ and the cavity (jet) luminosity L_{cav} is expressed in units of $10^{42} \text{ erg s}^{-1}$. From this relation, and with $L_{1.4 \text{ GHz}} = 4.57 \times 10^{24} \text{ W Hz}^{-1}$ for MRC 0116+111 (Table 2), we obtain $L_j = 1.2 \times 10^{44} \text{ erg s}^{-1}$, which is consistent with the earlier ‘calorimetric’ estimate. Moreover, adopting $t_j = 10^7-10^8 \text{ yr}$, the same as the synchrotron age derived in Section 3.3, we estimate that the total energy content (enthalpy) of the bubble system is $\sim 4 \times (10^{58}-10^{59}) \text{ erg}$, which is less than our earlier estimate ($10^{60}-10^{61}$) erg, but we believe it represents best the situation in MRC 0116+111. However, the exact figure can only be obtained from the future X-ray observations of MRC 0116+111.

Indeed, both observations and theory suggest that the energy input from AGN into the cluster atmosphere at this rate is sufficient to heat it up and balance the cooling loss (Dalla Vecchia et al. 2004; Rafferty et al. 2006). This may even halt (or reduce drastically) the accretion flow of matter on to the SMBH in some systems (e.g. Cattaneo & Teyssier 2007) – thus cutting off the fuel supply to the ‘central engine’ and completing the negative feedback loop. We wonder, if this AGN mediated feedback process could also be at work in MRC 0116+111, giving rise to its relaxed, quiescent looking appearance? If confirmed with future X-ray observations, such large enthalpy of the bubble system in MRC 0116+111 would make it harbour one of the most energetic radio outbursts known, comparable to the energetics of the supercavities in MS 0735.6+7421 and Hydra clusters (McNamara et al. 2005; Wise et al. 2007).

The ultrasteep spectrum north-west bubble is located at a projected distance of $R \sim 100 \text{ kpc}$ from the central cD galaxy, which is inferred to be buoyantly rising in the ICM. We do not know how far back in time it was inflated and where was it injected into the ICM. Assuming that it was initially inflated rapidly by an AGN-fed radio jet near the cluster centre, and subsequently it detached and rose subsonically at $\sim 1/2$ the speed of sound $C_s = 717.6 [T/(2 \text{ keV})]^{1/2} \text{ km s}^{-1}$, it will take $t_{s/2} = 2C_s^{-1}R = 2.7 \times 10^8 \text{ yr}$ for it to arrive at its present location (neglecting projection effects). This time-scale is much longer than the electron cooling time-scale $t_{\text{cool}} \approx 2 \times 10^7 \text{ yr}$ (taking $B = 10 \mu\text{G}$) at 4.86 GHz, thus consistent with its observed very steep radio spectrum (Fig. 6). However, the actual rise time should be somewhat shorter than the above estimate when we take into account the initial rapid inflation and acceleration phase (due to forward momentum of the radio jet), at the end of which the bubble will attain a constant terminal speed v_{term} and rise in pressure balance with the external medium. Another relevant time-scale is the ‘buoyant rise’ time t_{buoy} , which is the travel time for a bubble moving with the terminal speed v_{term} . The X-ray data show that usually $t_{\text{buoy}} \sim 2 \times t_{s/2}$ (Birzan et al. 2004; Wise et al. 2007).

Several galaxy clusters also show X-ray surface brightness depressions that have no obvious association with bright radio emission – the so-called ‘ghost cavities’, such as those seen in Abell 2597 (McNamara et al. 2001), and the matched pair of cavities in Hydra and Perseus clusters (Fabian et al. 2000; Wise et al. 2007). These depressions are thought to have been created by AGN outbursts that occurred in the more distant past, but whose radio emission has faded over time due to radiation and expansion losses (e.g. Ensslin & Gopal-Krishna 2001). An interesting possibility, suggested by our discovery of an ultrasteep spectrum detaching radio bubble in MRC 0116+111 is that such buoyantly rising radio bubbles are precursors of the ghost cavities observed in many X-ray observations. Such ghost bubbles provide important clues for understanding how AGNs heat cluster atmospheres. A crucial issue is the survival of detached radio bubbles up to large distances from the central source. The stability and dynamics of radio bubbles, once the jets have turned off (as in the present radio-halo MRC 0116+111), is a topic of great importance for the interpretation of X-ray observations of clusters. *Chandra* observations show that some of the ghost cavities are able to reach $\sim 20-100 \text{ kpc}$ distances from the central AGN, while it is found in several numerical simulations that hot thermal bubbles, once released into the cluster atmosphere at the end of a terminating radio jet, initially rise supersonically but are rapidly fragmented by Rayleigh–Taylor (RT) and Kelvin–Helmholtz (KH) instabilities. To prevent their destruction, the role of magnetic field in stabilization of the rising bubbles was explored by De Young (2003). Numerical simulations (e.g. Ruszkowski et al. 2008) find

that in an upward-rising cosmic ray filled bubble, the magnetic field ‘draping’ effect at the upper contact surface of bubble indeed has a strong stabilizing effect which prevents cross-field diffusion of particles. A substantial fraction of cosmic rays can thus be confined inside the bubbles on buoyant rise time-scales ($\sim 10^{7-8}$ yr) even when the parallel diffusivity coefficient is very large. Magnetic field stabilization of the radio bubbles in MRC 0116+111 is an interesting possibility worth exploring, as these are still intact quite far away from the central cD: ~ 100 kpc for north-west bubble and ~ 40 kpc for south-east bubble, requiring some stabilizing mechanism for their survival. Detailed polarization mapping of these features is required to check if the theoretical ‘draped’ structure of protecting magnetic field does exist.

Lastly, MRC 0116+111, with its dual bubble-like miniradio-halo morphology, provides an excellent test bed for understanding the dynamics of radio jet inflated buoyant plasma bubbles in the hot cluster atmospheres, and the role of AGN feedback in transporting and mixing of metals in the ICM. Low-entropy, metal-enriched cold gas may be uplifted from the cluster centre along with the energetic wakes of AGN-driven plasma bubbles up to $\sim 10-100$ kpc scales, which undergoes heating and mixing with ICM via hydrodynamical turbulence. Recently, from *Hubble Space Telescope (HST)* observations Fabian et al. (2008) discovered an extensive network of H α emitting cold, apparently magnetically supported, filaments surrounding the miniradio-halo Perseus A. They inferred that these cold filaments are dredged up from the centre of the galaxy by the radio-emitting bubbles, buoyantly rising in the hot intracluster gas, and act as markers of the AGN feedback process.

We expect that future more detailed radio, X-ray, γ -ray and optical emission line studies of the galaxy cluster hosting MRC 0116+111 would provide crucial data that would allow us to gain a much better understanding of the complex thermal and non-thermal plasma processes taking place in the gaseous environment around this puzzling yet extremely interesting radio-halo source.

5 SUMMARY AND CONCLUSIONS

(i) We have presented detailed radio and optical observations of MRC 0116+111, which clearly have revealed a luminous, steep-spectrum, diffuse radio-halo source of ~ 240 -kpc dimension located at the centre of a X-ray weak, low-mass cluster of galaxies at redshift $z = 0.131$.

(ii) On larger scales (~ 100 kpc) the radio-halo emission composed of two diffuse ‘lobe’-like structures surrounding the central cD and its associated group of galaxies, which we have interpreted as being a pair of radio emitting giant plasma bubbles, filled with relativistic particles (cosmic rays) and magnetic field.

(iii) We do not detect any ongoing AGN activity, such as a compact core or active radio jets feeding the plasma bubbles. Thus, it is possible that these bubbles are tracers of a previous cycle of AGN activity and were inflated by the pressure of radio jets in a highly energetic episode of AGN outburst, which has either ceased by now, or has become too feeble to be detectable.

(iv) The physical size, radio spectral index and morphology of MRC 0116+111 are broadly consistent with the properties of a cluster radio minihalo, which are rare objects, have low surface brightness and possess a steep spectral index ($\alpha \lesssim -1$). They are mostly observed at the centres of cooling-core clusters, which indicate that their origin and evolution are closely linked to the energy feedback from the central AGN via radio jets into ICM and its cool-

ing/heating processes. The radio luminosity of MRC 0116+111 at 1.4 GHz, 4.57×10^{24} W Hz $^{-1}$, and the bolometric radio luminosity (over 10 MHz–10 GHz range), 3.64×10^{34} W, would place it amongst the most luminous radio haloes known.

(v) The integrated radio spectrum shows a sudden steepening beyond the ‘break’ frequency ~ 400 MHz. The low-frequency spectral index is $-0.55(\pm 0.05)$ and the high-frequency spectral index is $-1.35(\pm 0.06)$. The electron spectral age was derived to be $(1.33-0.64) \times 10^8$ yr, for magnetic field values 1–10 μG .

(vi) The pair of huge (~ 100 kpc scale) plasma bubbles shows marked spectral index differences. Between 240 and 621 MHz (GMRT) both bubbles show a similar mean spectral index $\alpha_{\text{mean}} \approx -1$, indicating a lack of strong radiative losses. However, whereas between 1.4 and 4.8 GHz (VLA) the south-eastern bubble still has the same mean spectral index of $\alpha_{\text{mean}} = -1.06 \pm 0.15$, the north-west bubble, in contrast, has developed an extremely steep spectrum $\alpha_{\text{mean}} = -1.6 \pm 0.20$, clearly due to strong radiative energy losses. We argued that ongoing *in situ* particle re-acceleration, probably via merger-induced shocks and/or turbulence, is taking place in the south-eastern bubble, and the north-western bubble is detaching and buoyantly rising away from the centre in the hot cluster atmosphere. Such uprising, ageing bubbles are potential precursors of the giant X-ray dark cavities and could inject $\sim 10^{60-62}$ erg mechanical energy into the ICM for heating it, as observed in X-ray observations of several clusters.

(vii) We discovered a remarkable morphological similarity between MRC 0116+111 and M87, the well-known dominant central radio galaxy in the Virgo cluster. Similar internal plasma outflow structures and network of magnetic filaments surrounded by a pair of giant outer radio bubbles are observed. This suggests that both these sources might have originated in, and their evolution governed by, similar physical processes and conditions prevailing in the central regions of their host clusters. In spite of the notable similarities, at ~ 240 kpc, the linear size of MRC 0116+111 is about three times larger than M87. The bolometric radio luminosity of both is about same: 3.6×10^{34} W. This in turn implies that the average volume emissivity of MRC 0116+111 is roughly a factor of 30 smaller than that of M87 halo.

(viii) From the known empirical correlation between the estimated mechanical jet luminosities of radio AGNs that have associated X-ray cavities, and their 1.4 GHz monochromatic radio luminosities, we estimated the total enthalpy (free energy) of bubbles in MRC 0116+111, $\sim 10^{59-60}$ erg, and the mechanical luminosity of radio jets which inflated them, to be $\sim 10^{44}$ erg s $^{-1}$. Energy input from a central AGN into the cluster atmosphere at this rate is sufficient to heat it up, drive a massive outflow from the AGN, which may counter balance a possible cooling loss, and may even halt (or reduce drastically) the accretion flow of matter on to the SMBH, thus cutting off the fuel supply powering the central engine and completing the feedback loop. This AGN mediated feedback process in MRC 0116+111 could explain its relaxed, quiescent looking appearance. If confirmed with future X-ray observations, such large enthalpy of the bubble system in MRC 0116+111 and its possible AGN-feedback cycle would make it host one of the most energetic radio outbursts known, comparable to the energetics of the supercavities in MS 0735.6+7421 and Hydra clusters.

(ix) MRC 0116+111, with its rare, twin bubble-like morphology of miniradio halo and possessing other striking properties as revealed in our observations, provides an excellent opportunity to understand the energetics and the dynamical evolution of radio jet inflated plasma bubbles in the hot cluster atmosphere. It also helps in understanding what possible role AGN-feedback plays in heating of

ICM, transporting and mixing of metals in the ICM, the evolution of central galaxies and the growth of nuclear SMBHs.

ACKNOWLEDGMENTS

We thank the operations team of the NCRA–TIFR GMRT Observatory and IUCAA Girawali Observatory. We specially wish to thank Vijay Mohan (IUCAA) for providing extensive help during optical observation and data analysis and Hans Böhringer (MPE) for providing us with an upper limit on the X-ray luminosity of the source from the *ROSAT* All Sky Survey. We thank Frazer Owen (NRAO) for allowing us to use the VLA 90 cm image of M87. J. Jacob, N. Wadnerkar, J. Belapure and A. C. Kumbharkhane thank IUCAA for facilities and local support during several academic visits. NW was supported by the National Aeronautics and Space Administration (NASA) through *Chandra* Postdoctoral Fellowship Award Number PF8-90056 issued by the *Chandra X-Ray Observatory Center*, which is operated by the Smithsonian Astrophysical Observatory for and on behalf of the National Aeronautics and Space Administration under contract NAS8-03060.

REFERENCES

- Aharonian F. A., 2002, MNRAS, 332, 215
 Allen S. W., Dunn R. J. H., Fabian A. C., Taylor G. B., Reynolds C. S., 2006, MNRAS, 372, 21
 Baars J. W. M., Genzel R., Pauliny-Toth I. I. K., Witzel A., 1977, A&A, 61, 99
 Bagchi J., Kapahi V. K., 1994, JA&A, 15, 275
 Bagchi J., Durret F., Lima Neto G. B., Paul S., 2006, Sci, 314, 791
 Becker R. H., White R. L., Edwards A. L., 1991, ApJS, 75, 1
 Begelman M. C., Blandford R. D., Rees M., 1984, Rev. Mod. Phys., 56, 255
 Binney J., Tabor J., 1995, MNRAS, 276, 663
 Birzan L., Rafferty D. A., McNamara B. R., Wise M. W., Nulsen P. E. J., 2004, ApJ, 607, 800
 Birzan L., McNamara B. R., Nulsen P. E. J., Carilli C. L., Wise M. W., 2008, ApJ, 686, 859
 Blanton E. L., Sarazin C. L., McNamara B. R., Wise M. W., 2003, ApJ, 558, L15
 Böhringer H., Matsushita K., Churazov E., Ikebe Y., Chen Y., 2002, A&A, 382, 804
 Brüggen M., Kaiser C. R., 2002, Nat, 418, 301
 Brüggen M., Kaiser C. R., Churazov E., Ensslin T. A., 2002, MNRAS, 331, 545
 Brunetti G. et al., 2008, Nat, 455, 944
 Burns J. O., 1994, AJ, 99, 14
 Canizares C. R., Clark G. W., Jernigan J. G., Markert T. H., 1982, ApJ, 262, L32
 Cassano R., Gitti M., Brunetti G., 2008, A&A, 486, L31
 Cattaneo A., Teyssier R., 2007, MNRAS, 376, 1547
 Churazov E., Bruggen M., Kaiser C. R., Böhringer H., Forman W., 2001, ApJ, 554, 261
 Churazov E., Sunyaev R., Forman W., Böhringer H., 2002, MNRAS, 332, 729
 Cohen A. S., Lane W. M., Cotton W. D., Kassim N. E., Lazio T. J. W., Perley R. A., Condon J. J., Erickson W. C., 2007, AJ, 134, 1245
 Colafrancesco S., Blasi P., 1998, ApJ, 9, 227
 Condon J. J., Cotton W. D., Greisen E. W., Yin Q. F., Perley R. A., Taylor G. B., Broderick J. J., 1998, AJ, 115, 1693
 Dalla Vecchia C., Bower R. G., Theuns T., Balogh M. L., Mazzotta P., Frenk C. S., 2004, MNRAS, 355, 995
 De Young D. S., 2003, MNRAS, 343, 719
 Dunn R. J. H., Fabian A. C., 2004, MNRAS, 355, 862
 Dunn R. J. H., Fabian A. C., 2006, MNRAS, 373, 959
 Edge A. C., 2001, MNRAS, 328, 762
 Ensslin T. A., Gopal-Krishna, 2001, A&A, 366, 26
 Ensslin T. A., Biermann P. L., Kronberg P. P., Wu X.-P., 1997, ApJ, 477, 560
 Fabian A. C., 1994, ARA&A, 32, 277
 Fabian A. C. et al., 2000, MNRAS, 318, L65
 Fabian A. C., Sanders J. S., Allen S. W., Crawford C. S., Iwasawa K., Johnstone R. M., Schmidt R. W., Taylor G. B., 2003, MNRAS, 344, 43
 Fabian A. C., Johnstone R. M., Sanders J. S., Conselice C. J., Crawford C. S., Gallagher J. S., III, Zweibel E., 2008, Nat, 454, 968
 Feretti L., Giovannini G., 2008, in Plionis M., Lopez-Cruz O., Hughes D., eds, Lecture Notes in Physics, Vol. 740, A Pan-Chromatic View of Clusters of Galaxies and the Large-Scale Structure. Springer-Verlag, Dordrecht, p. 143
 Ferrari C., Govoni F., Schindler S., Bykov A. M., Rephaeli Y., 2008, Space Sci. Rev., 134, 93
 Ghizzardi S., Molendi S., Pizzolato F., 2004, ApJ, 609, 638
 Giovannini G., Feretti L., 2000, New Astron., 5, 335
 Gitti M., Brunetti G., Feretti L., Setti G., 2004, A&A, 417, 1
 Gitti M., Feretti L., Schindler S., 2006, A&A, 448, 853
 Gitti M., Ferrai C., Domainko W., Feretti L., Schindler S., 2007, A&A, 470, L25
 Gopal-Krishna, Kulkarni V. K., Bagchi J., Melnik J., 2002, in Rao A. P., Swarup G., Gopal-Krishna, eds, Proc. IAU Symp. 199, The Universe at Low Radio Frequencies. Astron. Soc. Pac., San Francisco, p. 159
 Govoni F., Feretti L., 2004, Int. J. Mod. Phys. D, 13, 1549
 Gull S. F., Northover K. J. E., 1973, Nat, 244, 80
 Harms R. J. et al., 1994, ApJ, 435, L35
 Heckman T. M., 1981, ApJ, 250, L59
 Hinton J. A., Domainko W., Pope C. D., 2007, MNRAS, 382, 466
 Jamrozy M., Klein U., Mack K.-H., Gregorini L., Parma P., 2004, A&A, 427, 79
 Joshi M. N., Singal A. K., 1980, Mem. Astron. Soc. India, 1, 49
 Landolt A. U., 1992, AJ, 104, 340
 Large M. I., Mills B. Y., Little A. G., Crawford D. F., Sutton J. M., 1981, MNRAS, 194, 693
 Loeb A., Waxman E., 2000, Nat, 405, 156
 Lopes P. A. A., de Carvalho R. R., Gal R. R., Djorgovski S. G., Odewahn S. C., Mahabal A. A., Brunner R. J., 2004, AJ, 128, 1017
 McNamara B. R., Nulsen P. E. J., 2007, ARA&A, 45, 117
 McNamara B. R., O'Connell R. W., 1989, AJ, 98, 2018
 McNamara B. R. et al., 2000, ApJ, 534, L135
 McNamara B. R. et al., 2001, ApJ, 562, L149
 McNamara B. R., Nulsen P. E. J., Wise M. W., Rafferty D. A., Carilli C., Sarazin C. L., Blanton E. L., 2005, Nat, 433, 45
 Mittal R., Hudson D. S., Reiprich T. H., Clarke T., 2009, A&A, 501, 835
 Murgia M., Govoni F., Markevitch M., Feretti L., Giovannini G., Taylor G. B., Carretti E., 2009, A&A, 499, 679
 Owen F. N., Eilek J. E., Kassim N. E., 2000, ApJ, 543, 611
 Parma P., Murgia M., de Ruiter H. R., Fanti R., Mack K.-H., Govoni F., 2007, A&A, 470, 875
 Pedlar A., Ghatare H. S., Davies R. D., Harrison B. A., Perley R., Crane P. C., Unger S. W., 1990, MNRAS, 246, 477
 Peterson J. R., Fabian A. C., 2006, Phys. Rep., 427, 1
 Pfrommer C., Ensslin T. A., 2004, A&A, 413, 17
 Rafferty D. A., McNamara B. R., Nulsen P. E. J., Wise M. W., 2006, ApJ, 652, 216
 Reiprich T. H., Böhringer H., 2002, ApJ, 567, 716
 Ruszkowski M., Ensslin T. A., Bruggen M., Begelman M. C., Churazov E., 2008, MNRAS, 383, 1359
 Ryu D., Kang H., Hallman E., Jones T. W., 2003, ApJ, 593, 599
 Salome P., Combes F., Revaz Y., Edge A. C., Hatch N. A., Fabian A. C., Johnstone R. M., 2008, A&A, 484, 317
 Sanders J. S., Fabian A. C., 2007, MNRAS, 381, 1381
 Slee O. B., Roy A. L., Murgia M., Andernach H., Ehle M., 2001, AJ, 122, 1172

- Soker N., Sarazin C. L., 1990, ApJ, 348, 73
Stanek R., Evrard E. E., Böhringer H., Schuecker P., Nord B., 2006, ApJ, 648, 956
Swarup G., Ananthakrishnan S., Kapahi V. K., Rao A. P., Subrahmanya C. R., Kulkarni V. K., 1991, Curr. Sci., 60, 95
Venturi T., Giacintucci S., Dallacasa D., Cassano R., Brunetti G., Bardelli S., Setti G., 2008, A&A, 484, 327
Völk H. J., Aharonian F. A., Breitschwerdt D., 1996, Space Sci. Rev., 75, 279
Wise M. W., McNamara B. R., Nulsen P. E., Houck J. C., David L. P., 2007, ApJ, 659, 1153

This paper has been typeset from a $\text{\TeX}/\text{\LaTeX}$ file prepared by the author.